RSC Advances

PAPER

View Article Online
View Journal | View Issue

Cite this: *RSC Adv.*, 2016, **6**, 58831

Catecholase and phenoxazinone synthase activities of a ferromagnetically coupled tetranuclear Cu(II) complex†

Merry Mitra,[a] Tanay Kundu,‡[b] Gurpreet Kaur,§[c] Gyaneswar Sharma,[d] Angshuman Roy Choudhury,[c] Yogesh Singh[d] and Rajarshi Ghosh*[a]

Received 3rd May 2016
Accepted 13th June 2016

DOI: 10.1039/c6ra11433d

www.rsc.org/advances

A crystallographically characterized tetranuclear Cu(II) complex $[Cu^{II}_4(L)_4]$ (**1**) [H_2L = *N*-(2-hydroxyethyl)-3-methoxysalicylaldimine] is found to show overall ferromagnetic exchange coupling. Complex (**1**) mimics the catalytic activity of the plant enzyme catechol oxidase by oxidising 3,5-di-*tert*-butylcatechol to its corresponding quinone in methanol and dichloromethane medium in the presence of aerial oxygen. The reaction follows Michaelis–Menten enzymatic reaction kinetics with turnover numbers (K_{cat}) 6.99 × 10^3 and 1.85 × 10^3 h^{-1} in methanol and dichloromethane, respectively. **1** is also phenoxazinone synthase active in methanol medium with a turnover number of 1.21 × 10^5 h^{-1}.

Introduction

High nuclearity transition-metal complexes are of current interest for their possible utility in molecular magnetism[1] with special emphasis on single molecule magnets.[2] The study of spin–spin interactions between paramagnetic metal centres has become one of the most important research areas in inorganic as well as coordination chemistry. Copper has long been the metal of choice for assembling high nuclearity clusters[3,4] primarily based on ligands with oxygen along with nitrogen donor atoms.

Enzymes that are capable of processing molecular oxygen under ambient conditions are being paid considerable attention now-a-days because complexes modeling their active site[5] may serve as efficient, mild catalysts to carry out synthetic organic transformations of industrial importance.[6] Dinuclear copper complexes play an important role in biological metalloenzymes.[7] Catechol oxidase, the plant enzyme which converts catechol to quinone coupled with the 2e/2H^+ reduction of oxygen to water in the presence of aerial oxygen, (Scheme 1) has a dinuclear hydroxobridged antiferromagnetically coupled Cu(II) active site.[8–10] They may have important physiological roles in photosynthesis, flower colouration and plant disease resistance.[8] As soon as the crystal structure of the active site of catecholase was published, a good number of copper complexes with different nuclearity appeared in the literature.[5c,11–14]

Phenoxazinone synthase, another multicopper oxidase, naturally produced by *Streptomyces antibioticus* which has been cloned and over-expressed in *S. lividians* is responsible for the six electron oxidative coupling of two molecules of an *o*-aminophenol (OAPH) derivative, 4-methyl-3-hydroxyanthraniloyl pentapeptide, to form the phenoxazinone chromophore[15] (Scheme 2) of the antineoplastic agent actinomycin D which is clinically used for the treatment of Wilm's tumor, gestational choriocarcinoma and other tumors. Few recent reports are found in modeling the phenoxazinone synthase.[16]

In the present report we have synthesized a tetranuclear copper(II) complex $[Cu^{II}_4(L)_4]$ (**1**) [H_2L = *N*-(2-hydroxyethyl)-3-methoxysalicylaldimine] which acts as a model for catechol oxidase and phenoxazinone synthase, and shows overall

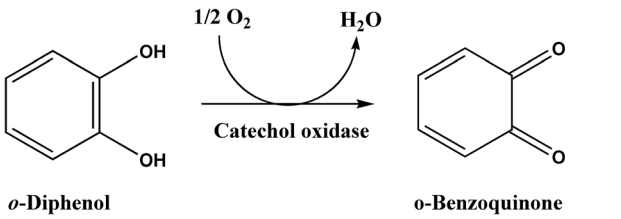

Scheme 1 Catecholase activity.

[a]Department of Chemistry, The University of Burdwan, Burdwan 713 104, India. E-mail: rghosh@chem.buruniv.ac.in
[b]Physical/Materials Chemistry Division, National Chemical Laboratory, Pune 411 008, India
[c]Department of Chemical Sciences, Indian Institute of Science Education & Research, Mohali, Sector 81, S.A.S. Nagar, Knowledge City, Manauli PO, Mohali 140 306, India
[d]Department of Physical Sciences, Indian Institute of Science Education & Research, Mohali, Sector 81, S.A.S. Nagar, Knowledge City, Manauli PO, Mohali 140 306, India

† Electronic supplementary information (ESI) available: UV-Vis, NMR, ESI-MS, HRMS and EPR data and are reported here. CCDC 1455999. For ESI and crystallographic data in CIF or other electronic format see DOI: 10.1039/c6ra11433d

‡ Present address: Institut Lavoisier, UMR CNRS 8180, Université de Versailles Saint-Quentin-en-Yvelines, 45 avenue des Etats-Unis, 78035 Versailles cedex, France.

§ Present address: Department of Chemistry, DAV University, Jalandhar, Punjab, 144 012, India.

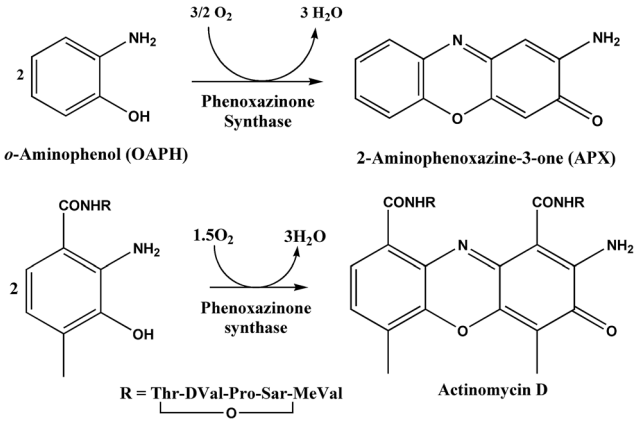

Scheme 2 Phenoxazinone synthase activity.

ferromagnetic exchange. The mechanistic aspect of this activity is also tried to be unraveled with experimental support. The X-ray structure similar, but not identical to **1** is found in recent literature.[17]

Results and discussion

Synthesis and formulation

Complex **1** was synthesized by addition of solid Cu(II) acetate dihydrate into the dichloromethane–acetonitrile mixture solution of the ligand H_2L.

The reaction is scheme is here:

$$2Cu_2(CH_3COO)_4\cdot 2H_2O + 4H_2L \rightarrow [Cu^{II}_4(L)_4] + 8CH_3COOH + 4H_2O$$

The complex was soluble in methanol and was characterized by spectroscopy, ESI-mass spectrometry and single-crystal X-ray crystallography. In the IR spectra, relatively intense peaks around 1590–1600 cm^{-1} due to the C=N stretching frequency appears the complex.

Crystallography

Single crystal X-ray crystallographic analysis of **1** was carried out on a Bruker SMART APEX II CCD diffractometer using Mo-Kα radiation ($\lambda = 0.71073$ Å). Diffraction data was collected at 100.0 (2) K and was identified as $P\bar{1}$ space groups. The crystal data and refinement details are listed in Table 1. The structure was solved by direct methods, and the structure solution and refinement were based on $|F|^2$. All calculations were carried out using SHELXL-97 (ref. 18) and were refined using SHELSL-97.[19] All the figures have been generated using ORTEP-32.[20]

Crystal structure of **1** is shown in Fig. 1 while selected bond angles and distances are given in Table 2. The crystal structure of the compound reveals that it is a tetranuclear Cu(II) complex with tetracoordination at each Cu centre. Each metal centre is coordinated with an imine, a phenoxo and one sharing alkoxo group from a single ligand backbone and the fourth coordination site is satisfied by another sharing alkoxo group from another ligand molecule in the complex. From bond angles and distances data (Table 2), it appears that each copper(II) centre is in distorted square planar geometry. The distortion occurs due to puckered structure of the ligand.

Table 1 Crystal data and structure refinement parameters for **1**

Empirical formula	$C_{40}H_{44}N_4O_{12}Cu_4$
Formula weight	1068.00
T (K)	100.0(2)
Wavelength (Å)	0.71073
Crystal system	Triclinic
Space group	$P\bar{1}$
Unit cell dimensions	
a (Å)	11.9179(14)
b (Å)	12.1517(14)
c (Å)	15.1464(18)
α (°)	102.667(2)
β (°)	92.928(2)
γ (°)	100.128(1)
V (Å^3)	2097.6(4)
Z	2
D_{calc} (mg m^{-3})	1.691
Absorption coefficient (mm^{-1})	2.071
F(000)	1092.0
Crystal size (mm^3)	0.2 × 0.1 × 0.1
Theta range for data collection (°)	1.384–25.027
Index ranges	$-14 \le h \le 13$, $-14 \le k \le 14$, $-18 \le l \le 17$
Reflections collected	21 470
Independent reflections	7373 [$R_{int} = 0.0248$]
Completeness to theta	0.994
Absorption correction	Multi-scan
T_{max} and T_{min}	0.7455 and 0.7030
Refinement method	Full-matrix least-squares on F^2
Data/restraints/parameters	7373/0/573
Goodness-of-fit (GOF) on F^2	1.047
Final R indices [$l > 2\sigma(l)$]	$R_1 = 0.0272$, w$R_2 = 0.0680$
R indices (all data)	$R_1 = 0.0345$, w$R_2 = 0.0644$
Largest difference in peak and hole (e Å^{-3})	0.629, −0.324

Magnetism

The χ *vs.* T data are shown in Fig. 2. To extract the nature and magnitude of magnetic interactions in the system we have analyzed the χ data using the Curie–Weiss model for which the susceptibility in the paramagnetic state is given by the expression $\chi = \chi_0 + C/(T - \theta)$, where χ_0 is the temperature independent contribution, C is the Curie constant which depends on the effective magnetic moment, and θ is the Weiss temperature, the sign and magnitude of which will give the nature of the magnetic exchange interactions. For small χ_0, this will lead to $1/\chi$ being linear. The $1/\chi$ *vs.* T data are shown in the inset (a) of Fig. 2. It can be seen that at high temperatures, the behavior is linear as expected. The high temperature data between $T = 200$ K to 300 K data were fit to the above Curie–Weiss expression. The parameters obtained from the fit are $\chi_0 = 1.17(3) \times 10^{-4}$ cm^3 per Cu mol, $C = 0.435(7)$ cm^3 K per Cu mol, and $\theta = 16.6$ K. From C, the effective moment μ_{eff} can be estimated using the expression $C = N_A\mu_{eff}^2/3k_BT$, where N_A is the Avogadro's number

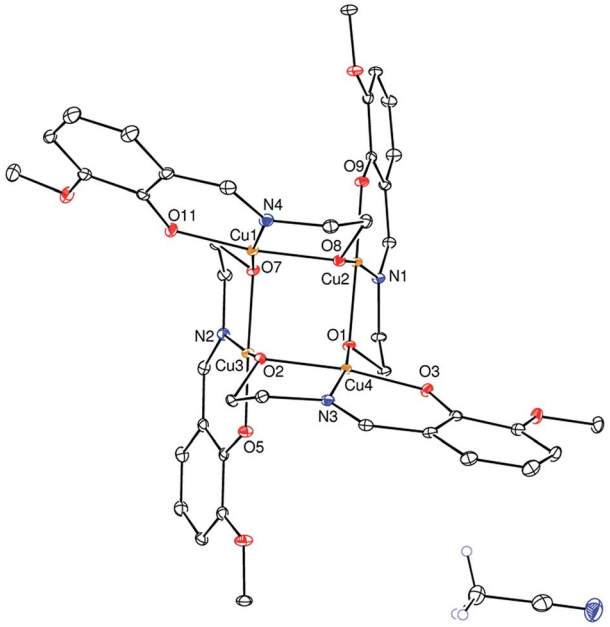

Fig. 1 An ORTEP of $[Cu_4(L)_4]$ (**1**) with atom numbering scheme and 20% probability ellipsoids for all non-hydrogen atoms.

Table 2 Bond lengths [Å] and angles [°] for **1**

Bond lengths			
Cu(1)–O(7)	1.9457(17)	Cu(3)–O(2)	1.9536(16)
Cu(1)–O(8)	1.9851(18)	Cu(3)–O(5)	1.8936(18)
Cu(1)–O(11)	1.9056(19)	Cu(3)–O(7)	1.9651(17)
Cu(1)–N(4)	1.941(2)	Cu(3)–N(2)	1.936(2)
Cu(2)–O(1)	1.9748(17)	Cu(4)–O(1)	1.9406(15)
Cu(2)–O(8)	1.9551(16)	Cu(4)–O(2)	1.9763(17)
Cu(2)–O(9)	1.9116(17)	Cu(4)–O(3)	1.9005(18)
Cu(2)–N(1)	1.927(2)	Cu(4)–N(3)	1.936(2)
Bond angles			
O(7)–Cu(1)–O(8)	87.53(7)	O(5)–Cu(3)–O(7)	176.91(7)
O(7)–Cu(1)–O(11)	94.06(8)	N(2)–Cu(3)–O(2)	165.51(8)
O(8)–Cu(1)–O(11)	172.83(8)	N(2)–Cu(3)–O(5)	94.14(8)
N(4)–Cu(1)–O(7)	169.00(8)	N(2)–Cu(3)–O(7)	84.04(8)
N(4)–Cu(1)–O(8)	84.05(8)	O(1)–Cu(4)–O(2)	86.70(7)
N(4)–Cu(1)–O(11)	93.45(9)	O(1)–Cu(4)–O(3)	94.94(7)
O(1)–Cu(2)–O(8)	86.16(7)	O(2)–Cu(4)–O(3)	172.58(7)
O(1)–Cu(2)–O(9)	177.72(7)	N(3)–Cu(4)–O(1)	169.25(8)
O(8)–Cu(2)–O(9)	95.69(7)	N(3)–Cu(4)–O(2)	84.02(8)
N(1)–Cu(2)–O(1)	83.41(8)	N(3)–Cu(4)–O(3)	93.59(8)
N(1)–Cu(2)–O(8)	167.97(8)	Cu(1)–O(7)–Cu(3)	108.58(8)
N(1)–Cu(2)–O(9)	94.88(8)	Cu(3)–O(2)–Cu(4)	104.60(8)
O(2)–Cu(3)–O(7)	86.14(7)	Cu(4)–O(1)–Cu(2)	108.14(8)
O(2)–Cu(3)–O(5)	96.10(7)	Cu(2)–O(8)–Cu(1)	104.53(8)

and k_B is the Boltzmann constant. This gives $\mu_{eff} = 1.86(2)\ \mu_B$. The value expected for $S = 1/2$ magnetic moments is $\mu_{eff} = 1.73\ \mu_B$ assuming a g-factor of $g = 2$. A value $g = 2.1$ is enough to explain our slightly enhanced μ_{eff}.

Let us now turn to the nature of the magnetic exchange interactions between these $S = 1/2$ Cu moments. The value $\theta = 16.6$ K indicate moderate ferromagnetic coupling between the Cu ions. Evidence for this can also be seen in the χT data which

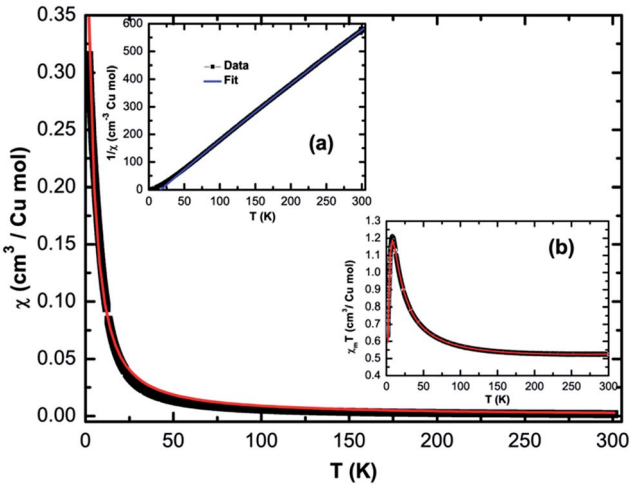

Fig. 2 Plots of χ *vs.* T for **1**; (a) $1/\chi$ *vs.* T plot; (b) χT *vs.* T plot showing value of $\theta = 16.6$ K indicating moderate ferromagnetic coupling between the Cu ions.

is shown in inset (b) of Fig. 2. χT, which is roughly the effective moment, is more or less T-independent for higher temperatures but increases dramatically as the temperature is lowered towards $T = \theta$. Normally, the system would undergo long-ranged ferromagnetic transition at this temperature. However, our system is more complex. It can be seen from inset (a) of Fig. 2 that the $1/\chi$ data deviate from the Curie–Weiss fit at lower temperatures. The $1/\chi$ becomes higher than expected from the fit, which in turn means that the χ becomes lower than expected for purely ferromagnetic interactions. This implies the presence of weak antiferromagnetic interactions which show up at much lower temperatures. Evidence for this can also be seen in the χT data which passes over a sharp maximum around $T = \theta$ before decreasing sharply for lower temperatures. Thus, our magnetic study reveals very complex magnetic interactions in this system with both ferromagnetic and antiferromagnetic interactions of different magnitudes present.

We propose that within a Cu_4 tetramer we have ferromagnetic exchange, while the inter-tetramer exchange is small and antiferromagnetic. With this preliminary information about the magnetic exchange interactions in the system we have analyzed the full χ *vs.* T data using an isotropic Heisenberg spin Hamiltonian given by,

$$H = -J_1(S_1S_2 + S_2S_3 + S_3S_4 + S_1S_4)$$

where J_1 is the ferromagnetic exchange between the spins S_i within one tetramer. Using the substitutions

$$S_A = S_1 + S_3,\ S_B = S_2 + S_4, \text{ and } S_T = S_A + S_B,$$

where S_T is the spin of the complete molecule, the Hamiltonian can be rewritten as

$$H = -J_1(S_1 + S_3)(S_2 + S_4) = -J_1S_AS_B = -J_1({S_T}^2 - {S_A}^2 - {S_B}^2)/2$$

The eigen values $E(S_T, S_A, S_B)$ are then given by,

$$E(S_T, S_A, S_B) = -J_1[S_T(S_T + 1) - S_A(S_A + 1) - S_B(S_B + 1)]/2$$

where $S_A = 0$ and 1, $S_B = 0$ and 1, and $S_T = 0$, 1, and 2. The magnetic susceptibility χ for a collection of Cu_4-tetramers, which can then be calculated using the Van Vleck equation, comes out to be

$$\chi_0 = \left(\frac{2N_A\mu_B{}^2g^2}{k_BT}\right)\left[\frac{2 + e^{\frac{J_1}{2T}} + 5e^{\frac{2J_1}{2T}}}{7 + 3e^{\frac{J_1}{2T}} + 6e^{\frac{2J_1}{2T}}}\right].$$

Assuming that the interactions between tetramers acts as a mean-field, the susceptibility of interacting tetramers can then be written down as

$$\chi = \left(\frac{\chi_0}{1 + \lambda\chi_0}\right),$$

where λ is the exchange coupling which can be given in terms of the inter-tetramer exchange J_2 as $\lambda = zJ_2/3C$, where $z = 6$ is the number of nearest neighbor tetramers and C is the Curie constant for $S = 1/2$. The experimental χ data were fit by the above theoretical expression. The fit, shown in Fig. 2 as the red curve through the data gave the values $J_1 = 33.0$ (4) K (*i.e.* 22.9 cm^{-1}) and $J_2 = -1.0$ (7) K (*i.e.* -0.6 cm^{-1}). The error factor came out to be $R = 1.31 \times 10^{-5}$. Similar exchange interactions are found in some of the recent literature.[17,21]

Catecholase activity

Spectrophotometric studies. The catecholase activity study was carried out using the substrate 3,5-di-*tert*-butyl catechol (3,5-DTBC) having two bulky *t*-butyl substituents on the ring and low quinone–catechol reduction potential. This makes it easily oxidized to the corresponding *ortho*-quinone derivative 3,5-di-*tert*-butyl quinone (3,5-DTBQ) which is highly stable and shows a maximum absorption at 401 nm in methanol.[11] Spectral bands at 666, 374, 278 and 234 nm appear in the electronic spectrum of complex **1**, whereas 3,5-DTBC shows a single band at 282 nm. Upon treatment of methanolic solution of **1** into 100 equivalents of 3,5-DTBC under aerobic conditions, the repetitive UV-Vis spectral scan was recorded (Fig. 3). The colourless solution gradually turned deep brown which indicates conversion of 3,5-DTBC to 3,5-DTBQ. In UV-Vis spectrophotometer, after this addition, the spectral scan shows very smooth increase of a quinone band at around ~390 nm which shifts ultimately to 401 nm, as reported by Krebs *et al.*[22] The same reaction was carried out by scaling up the reagents and 3,5-DTBQ was purified by column chromatography. It was then isolated and identified by H^1 NMR spectroscopy (Fig. S1; ESI†). H^1 NMR ($CDCl_3$, 400 MHz): $\delta_H = 1.16$ (s, 9H), 1.20 (s, 9H), 6.15 (d, $J = 2.4$ Hz, 1H), 6.86 (d, $J = 2.4$ Hz, 1H).

The time dependent change in absorbance at a wavelength of 401 nm, characteristic of 3,5-DTBQ in methanol, was observed for 25 min to comprehend the reaction kinetics and find out the reaction rate between 3,5-DTBC and **1**. The difference in absorbance ΔA at 401 nm, was plotted against time to obtain the rate/velocity for that particular catalyst to substrate concentration ratio (Fig. 4). A first-order catalytic reaction is observed, with rate 0.0211 min^{-1}.

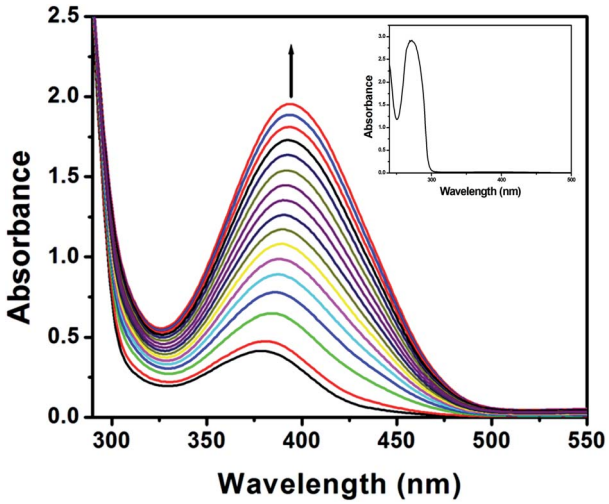

Fig. 3 Change in spectral pattern of complex **1** after reaction with 3,5-DTBC, observing the reaction for 6 h in methanol; inset: spectrum of pure 3,5-DTBC in methanol. This repetitive spectra were obtained in 9 min interval at room temperature. The peak for the coloured product (3,5-DTBQ) appears at ~390 nm which gradually shifts to 401 nm.[22]

The catecholase activity of complex **1** was similarly studied in DCM media. Similar to that of MeOH, in DCM also 3,5-DTBQ shows maximum absorption at ~390 nm which shifts to 401 nm finally (Fig. S2; ESI†). 3,5-DTBQ obtained, was purified by column chromatography and characterized by determining its melting point (~110 °C) which agreed well with that reported in literature.[23]

The reaction kinetics was studied by observing the time dependent change in absorbance at a wavelength of 401 nm for catalysis in dichloromethane. The difference in absorbance ΔA at these particular wavelengths, were plotted against time to

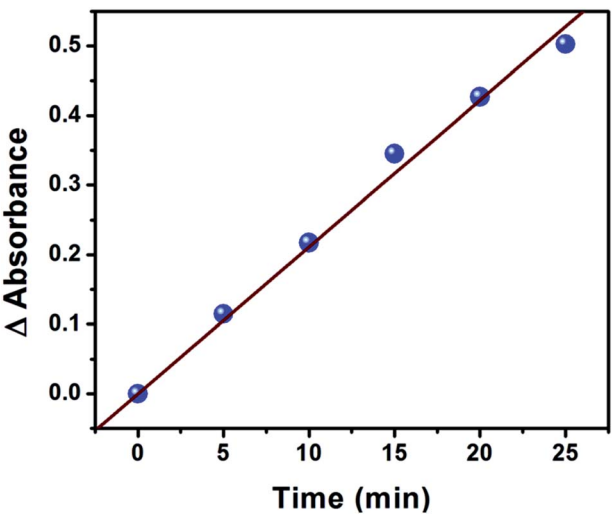

Fig. 4 A plot of the difference in absorbance (ΔA) *vs.* time to evaluate the rate of catalysis of 3,5-DTBC by **1** in methanol.

obtain the rate of the reaction. A first-order catalytic reaction with rate 5.95×10^{-3} min^{-1} is observed in DCM (Fig. S3; ESI†).

Enzyme kinetic study. Kinetic experiments were performed spectrophotometrically with complex **1** and the substrate 3,5-DTBC in methanol and dichloromethane, thermostated at 20 °C. 0.04 ml of the complex solution, with a constant concentration of 1×10^{-4} M, was added to 2 ml of 3,5-DTBC of a particular concentration (varying its concentration from 1×10^{-3} M to 1×10^{-2} M) to achieve the final concentration of the complex as 1×10^{-4} M. The conversion of 3,5-DTBC to 3,5-DTBQ was monitored with time at a wavelength of 401 nm for solutions in MeOH and DCM. The rate for each concentration of the substrate was determined by the initial rate method.

The rate *versus* concentration of substrate data were analyzed on the basis of Michaelis–Menten approach of enzymatic kinetics to get the Lineweaver–Burk (double reciprocal) plot as well as the values of the various kinetic parameters V_{max}, K_M and K_{cat}. The observed rate *vs.* [substrate] plot as well as Lineweaver–Burk plot in methanol and dichloromethane solutions are given in Fig. 5 and S4 (ESI†) respectively. The kinetic parameters are listed in Table 3. The turnover numbers (K_{cat}) are 6.99×10^3 and 1.85×10^3 h^{-1} in MeOH and DCM, respectively.

Reaction mechanism. The catalytic process follows a two-step mechanistic pathway. The first step is the rate determining step. Probably, in this step, the 1 : 1 adduct of catechol and the copper complex is formed. To obtain a mechanistic inference of the catecholase activity and to get an idea about the complex-substrate intermediate, we recorded an ESI-MS spectrum of **1** in methanol (Fig. S5a; ESI†) and of a 1 : 100 mixture of complex **1** and 3,5-DTBC of mixing them together (Fig. S5b; ESI†). The signal at $m/z = 196$ is due to the formation of the protonated ligand $[H_2L]$–H^+. The peak at $m/z = 243$ can be assigned to sodium aggregate of quinone [3,5-DTBQ]–Na^+. The protonated complex $[Cu_4(L)_4]$–H^+ exhibits a peak at $m/z = 1027$. The catalytic process is shown in Scheme 3. The formation of an complex-substrate adduct intermediate species is identified by the peak at $m/z = 477$. The semiquinone is identified from EPR spectrum (Fig. S6; ESI†). The catechol derivative, 3,5-DTBC gets oxidised to quinone in presence of oxygen. The aerial oxygen that oxidises 3,5-DTBC to 3,5-DTBQ in this process is converted to H_2O_2. H_2O_2 thus liberated was identified and characterized spectrophotometrically (S1; ESI†).[24]

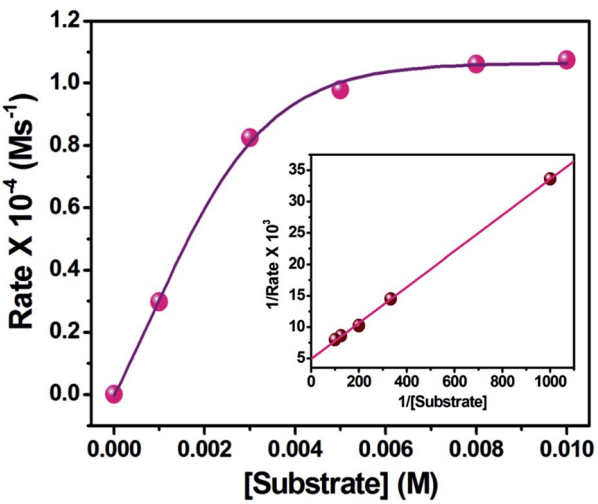

Fig. 5 Plot of rate *vs.* [substrate] (3,5-DTBC) in presence of 1 in MeOH; inset: Lineweaver–Burk plot.

Phenoxazinone synthase activity

Spectrophotometric studies. The phenoxazinone synthase activity study was carried out using the substrate *o*-aminophenol (OAPH). OAPH shows bands at 286 and 232 nm in pure methanol. Upon treatment of methanolic solution of **1** into 100 equivalents of OAPH under aerobic conditions, the repetitive

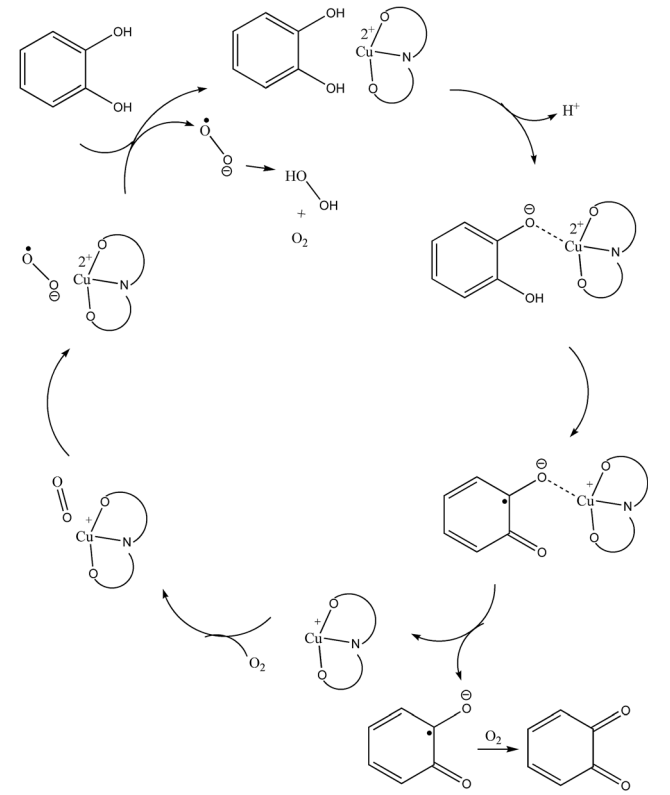

Scheme 3 Catalytic cycle for catecholase activity by **1**.

Table 3 Kinetic parameters for the oxidation of 3,5-DTBC catalyzed by 1

Solvent	V_{max} (M s^{-1})	Std. error	K_M (M)	Std. error	K_{cat} (h^{-1})
MeOH	1.94×10^{-4}	6.94×10^{-5}	5.39×10^{-3}	2.86×10^{-3}	6.99×10^3
DCM	5.14×10^{-5}	3.37×10^{-6}	4.04×10^{-4}	1.04×10^{-4}	1.85×10^3

UV-Vis spectral scan was recorded (Fig. 6). The colourless solution gradually turned deep brown which indicates conversion of OAPH to 2-aminophenoxazine-3-one (APX). The spectral scan shows very smooth growing of APX band at 427 nm.[16] APX was identified by HRMS with $m/z = 213$ (Fig. S7; ESI†). The time dependent change in absorbance at a wavelength of 427 nm, characteristic of APX in methanol, was observed for 25 min to comprehend the reaction kinetics and find out the reaction rate between OAPH and **1**. The difference in absorbance ΔA at 427 nm, was plotted against time to obtain the initial rate for that particular catalyst to substrate concentration ratio (Fig. 7). A first-order catalytic reaction is observed, with initial rate 0.0188 min^{-1}.

Enzyme kinetic study. Enzymatic kinetic experiments were performed UV-Vis spectrophotometrically thermostated at 25 °C with complex **1** and the substrate OAPH in MeOH. 0.04 ml of the complex solution, with a constant concentration of 1×10^{-4} M, was added to 2 ml of OAPH of a particular concentration (varying its concentration from 1×10^{-3} M to 1×10^{-2} M) to achieve the final concentration of the complex as 1×10^{-4} M. The conversion of OAPH to APX was monitored with time at a wavelength of 427 nm for solutions in MeOH. The rate for each concentration of the substrate was determined by the initial rate method. The rate *versus* concentration of substrate data were analyzed on the basis of Michaelis–Menten approach of enzymatic kinetics to get the Lineweaver–Burk (double reciprocal) plot as well as the values of the various kinetic parameters V_{max}, K_M and K_{cat}. The observed rate *vs.* [substrate] plot in methanol solution as well as Lineweaver–Burk plot is given in Fig. 8. The kinetic parameters are listed in Table 4. The turnover number (K_{cat}) is 1.21×10^5 h^{-1} in methanol.

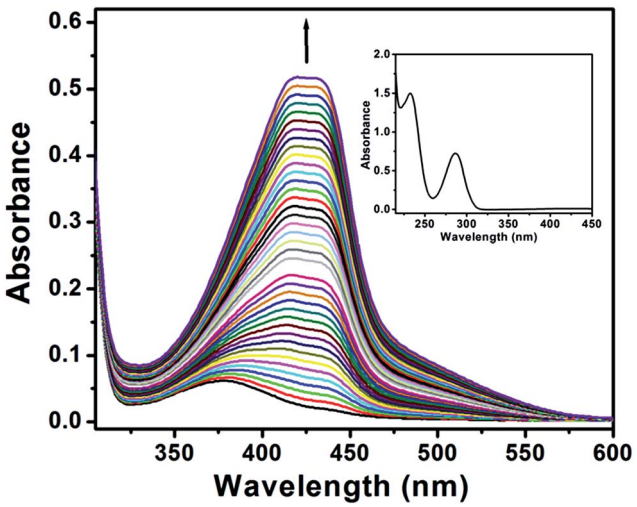

Fig. 6 Change in spectral pattern of complex **1** in MeOH after reaction with OAPH, observing the reaction for 6 h; inset: spectrum of pure OAPH in methanol.

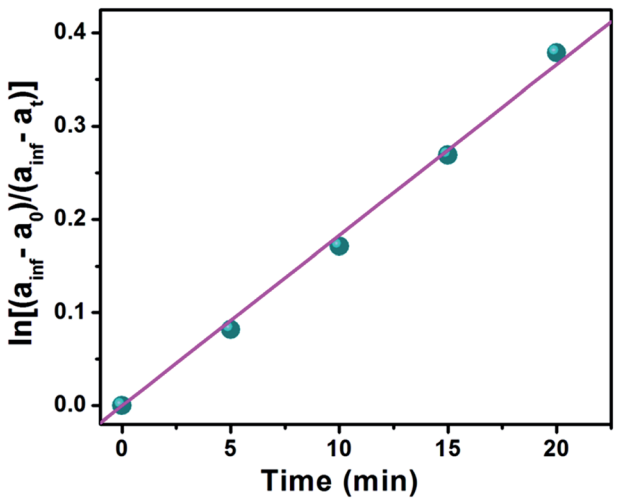

Fig. 7 A plot of the change in absorbance with time to evaluate the initial rate of the catalytic oxidation of OAPH by **1**.

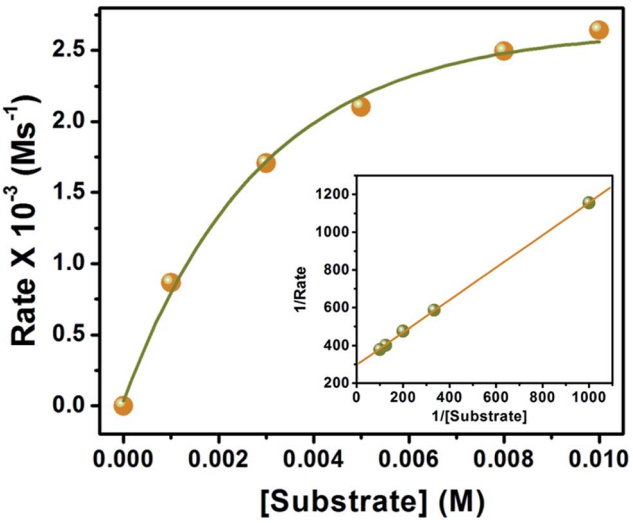

Fig. 8 Plot of rate *vs.* [substrate] (OAPH) in presence of **1** in MeOH; inset: Lineweaver–Burk plot.

Table 4 Kinetic parameters for the oxidative coupling of OAPH catalyzed by **1**

Solvent	V_{max} (M s^{-1})	Std. error	K_M (M)	Std. error	K_{cat} (h^{-1})
MeOH	3.36×10^{-3}	2.11×10^{-4}	2.89×10^{-3}	2.39×10^{-4}	1.21×10^5

Experimental

Materials and methods

High purity *o*-vanillin (Aldrich, UK), 2-aminoethanol (Aldrich, UK), copper(II) acetate dihydrate (Aldrich, UK), 3,5-di-*tert*-butylcatechol (Aldrich, UK), *o*-aminophenol (Aldrich, UK) and all other solvents were purchased from the respective concerns and used as received. Solvents were dried according to standard procedure and distilled prior to use.

The ligand H_2L was prepared using a reported procedure.[3a] *O*-vanillin (0.3043 g, 2 mmol) was heated under reflux with ethanol amine (0.1222 g, 2 mmol) in 30 ml dehydrated ethanol.

After 2 h, the reaction solution was evaporated under reduced pressure to yield a yellow coloured solid, which was dried under vacuum and stored over $CaCl_2$ for subsequent use.

For catecholase activity study, 1×10^{-4} mol dm^{-3} solution of **1** (0.0011 g) was treated with 1×10^{-2} mol dm^{-3} (100 equivalents) of 3,5-DTBC (0.0222 g) under aerobic conditions.

For phenoxazinone synthase activity study, 1×10^{-4} mol dm^{-3} solution of **1** (0.0011 g) was treated with 1×10^{-2} mol dm^{-3} (100 equivalents) of OAPH (0.0109 g) under aerobic conditions.

General procedure for synthesis of 1

Compound **1** was prepared by addition of solid $Cu_2(OAc)_4 \cdot 2H_2O$ (0.0498 g, 0.25 mmol) into a stirring solution of H_2L (0.0244 g, 0.125 mmol) in dichloromethane–acetonitrile mixture (15 ml). The resulting deep green coloured solution was kept in open air for slow evaporation. After 8–10 days, the deep green crystals of **1** was collected, washed with hexane and dried *in vacuo* over silica gel indicator.

Yield: (based on metal salt) 0.0562 g (84.25%). Anal. calc. for $C_{40}H_{44}N_4O_{12}Cu_4$ (**1**): C, 44.94; H, 4.15; N, 5.24; found: C, 39.97; H, 3.84; N, 3.82. Selected IR bands (KBr pellet, cm^{-1}): 3464 (s), 1637 (s), 1606 (s), 1473 (s) 1440 (s). UV-Vis (λ, nm): 666, 374, 278, 234.

Physical measurements

Elemental analyses (carbon, hydrogen and nitrogen) were performed on a Perkin-Elmer 2400 CHNS/O elemental analyzer. UV-Vis and IR spectra (KBr discs, 4000–300 cm^{-1}) were recorded using a Shimadzu UV-Vis 2450 spectrophotometer and Perkin-Elmer FT-IR model RX1 spectrometer, respectively. The H^1 NMR spectral data were collected in $CDCl_3$ on a Bruker 400 MHz spectrometer. Mass spectrometric data were collected on Waters Q-TOF-MICRO MS system using electron spray ionisation (ESI) techniques. Magnetic susceptibility χ *versus* temperature T measurements were performed on powder samples in an applied magnetic field of $H = 1$ T, using the VSM option of a Quantum Design PPMS.

Conclusions

Synthesis and crystallographic characterization of a tetranuclear Cu(II) Schiff base complex is reported here. The variable temperature magnetic measurement shows an overall ferromagnetic along with a weak antiferromagnetic interaction in the complex. The compound shows catecholase activity in methanol and dichloromethane solvent with turnover numbers 6.99×10^3 and 1.85×10^3 h^{-1}, respectively, which are much higher than those reported in recent times.[11b–d,24b] Mohanta *et al.* reported the turnover numbers 39 h^{-1}, 40 h^{-1}, and 48 h^{-1} in DMF, and 167 h^{-1} and 215 h^{-1} in MeCN for Cu(II) complexes.[11b] In a recent report by Rajak *et al.*, two Cu(II) complexes show a turnover rate of about 29 and 37 h^{-1}.[11c] The same group reported a dicopper complex with turnover number of 26 h^{-1}.[11d] A turnover rate of 28 h^{-1} of a Cu(II) complex is reported by Neves *et al.*[24b] The above results indicate that **1** is an effective model for catecholase activity than the recent reported ones, though, to the best of our knowledge, the most active catalyst[11a] reported so far, exhibits a turnover number of 3.24×10^4 h^{-1}. It is also phenoxazinone synthase active in methanol medium with a turnover number of 1.21×10^5 h^{-1}. So comparing all these data it can be concluded that the reported complex (**1**) is quite an efficient catalyst and has an appreciable turnover rates in various solvents.

Acknowledgements

RG sincerely thanks Department of Science & Technology, Government of West Bengal [No. 781(Sanc.)/ST/P/S&T/4G-4/2013 dated 04-12-2014], India for financial assistance. MM thanks The University of Burdwan for her fellowship. We extend our gratitude to Dr R. Banerjee, Physical/Materials Chemistry Division, National Chemical Laboratory, Pune 411 008, India for X-ray crystallographic studies.

Notes and references

1 (*a*) J. Hernández-Gil, N. Ovèjak, S. Ferrer, F. Lloret and A. Castiñeiras, *Inorg. Chem.*, 2013, **52**, 2289; (*b*) R. C. Poulten, M. J. Page, A. G. Algarra, J. J. Le Roy, I. López, E. Carter, A. Llobet, S. A. Macgregor, M. F. Mahon, D. M. Murphy, M. Murugesu and M. K. Whittlesey, *J. Am. Chem. Soc.*, 2013, **135**, 13640; (*c*) A. Aliev, M. Huvé, S. Colis, M. Colmont, A. Dinia and O. Mentré, *Angew. Chem., Int. Ed.*, 2012, **124**, 9527; (*d*) A. Mukherjee, R. Raghunathan, M. K. Saha, M. Nethaji, S. Ramasesha and A. R. Chakravarty, *Chem.–Eur. J.*, 2005, **11**, 3087.

2 (*a*) S. K. Langley, N. F. Chilton, B. Moubaraki and K. S. Murray, *Inorg. Chem.*, 2013, **52**, 7183; (*b*) A. Masello, K. A. Abboud, W. Wernsdorfer and G. Christou, *Inorg. Chem.*, 2013, **52**, 10414; (*c*) S.-D. Jiang, B.-W. Wang, G. Su, Z.-M. Wang and S. Gao, *Angew. Chem., Int. Ed.*, 2010, **122**, 7610.

3 (*a*) Y. Nishida and S. Kida, *J. Chem. Soc., Dalton Trans.*, 1986, 2633; (*b*) W. Mazurek, B. J. Kennedy, K. S. Murray, M. J. O'connor, J. R. Rodgers, M. R. Snow, A. G. Wedd and P. R. Zwack, *Inorg. Chem.*, 1985, **24**, 3258; (*c*) K. Geetha, M. Nethaji, N. Y. Vasanthacharya and A. R. Chakravarty, *J. Coord. Chem.*, 1999, **47**, 77.

4 (*a*) R. D. Harcourt, F. L. Skrezenek and R. G. A. R. Maclagan, *J. Am. Chem. Soc.*, 1986, **108**, 5403; (*b*) M. Kato and Y. Muto, *Coord. Chem. Rev.*, 1988, **92**, 45; (*c*) M. Melnik, *Coord. Chem. Rev.*, 1982, **42**, 259; (*d*) S.-F. Si, J.-K. Tang, D.-Z. Liao, Z.-H. Jiang and S.-P. Yan, *Inorg. Chem. Commun.*, 2002, **5**, 76.

5 (*a*) S. Majumder, S. Mondal, P. Lemoine and S. Mohanta, *Dalton Trans.*, 2013, **42**, 4561; (*b*) S. Mukherjee, T. Weyhermuller, E. Bothe, K. Wieghardt and P. Chaudhuri, *Dalton Trans.*, 2004, 3842; (*c*) S. Mandal, J. Mukherjee, F. Lloret and R. N. Mukherjee, *Inorg. Chem.*, 2012, **51**, 13148.

6 (*a*) S. Friedle, E. Reisner and S. J. Lippard, *Chem. Soc. Rev.*, 2010, **39**, 2768; (*b*) P. C. A. Bruijnincx, G. van Koten and

R. J. M. Klein Gebbink, *Chem. Soc. Rev.*, 2008, **37**, 2716; (*c*) S. I. Chan and S. S.-F. Yu, *Acc. Chem. Res.*, 2008, **41**, 969.

7 I. Bertini, H. H. Gray, S. J. Lippard and J. S. Valentine, *Bioinorganic chemistry*, Viva Books Pvt. Ltd., New Delhi, 1998.

8 C. Gerdemann, C. Eicken and B. Krebs, *Acc. Chem. Res.*, 2002, **35**, 183.

9 E. I. Solomon, U. M. Sundaram and T. E. Machonkin, *Chem. Rev.*, 1996, **96**, 2563.

10 (*a*) T. Klabunde, C. Eicken, J. C. Sacchettini and B. Krebs, *Nat. Struct. Biol.*, 1998, **5**, 1084; (*b*) C. Eicken, F. Zippel, K. Büldt-Karentzopoulos and B. Krebs, *FEBS Lett.*, 1998, **436**, 293; (*c*) A. Rompel, H. Fischer, D. Meiwes, K. Büldt-Karentzopoulos, R. Dillinger, F. Tuczek, H. Witzel and B. Krebs, *JBIC, J. Biol. Inorg. Chem.*, 1999, **4**, 56.

11 (*a*) K. S. Banu, T. Chattopadhyay, A. Banerjee, S. Bhattacharya, E. Suresh, M. Nethaji, E. Zangrando and D. Das, *Inorg. Chem.*, 2008, **47**, 7083; (*b*) S. Majumder, S. Sarkar, S. Sasmal, E. Carolina Sãnudo and S. S. Mohanta, *Inorg. Chem.*, 2011, **50**, 7540; (*c*) A. Banerjee, S. Sarkar, D. Chopra, E. Colacio and K. K. Rajak, *Inorg. Chem.*, 2008, **47**, 4023; (*d*) A. Banerjee, R. Singh, E. Colacio and K. K. Rajak, *Eur. J. Inorg. Chem.*, 2009, 277.

12 (*a*) K. Selmeczi, M. Reglier, M. Giorgi and G. Speier, *Coord. Chem. Rev.*, 2003, **245**, 191; (*b*) M. C. Mimmi, M. Gullotti, L. Santagostini, A. Saladino, L. Casella, E. Monzani and R. Pagliarin, *J. Mol. Catal. A: Chem.*, 2003, **204–205**, 381; (*c*) C. T. Yang, M. Vetrichelvan, X. Yang, B. Moubaraki, K. S. Murray and J. J. Vittal, *Dalton Trans.*, 2004, 113; (*d*) J. Reim and B. Krebs, *J. Chem. Soc., Dalton Trans.*, 1997, 37934; (*e*) L. González-Sebastián, V. M. Ugalde-Saldívar, E. Mijangos, M. R. Mendoza-Quijano, L. Ortiz-Frade and L. Gasque, *J. Inorg. Biochem.*, 2010, **104**, 1112; (*f*) L. Gasque, V. M. Ugalde-Saldívar, I. Membrillo, J. Olguín, E. Mijangos, S. Bernès and I. González, *J. Inorg. Biochem.*, 2008, **102**, 1227.

13 (*a*) A. L. Abuhijleh, J. Pollitte and C. Woods, *Inorg. Chim. Acta*, 1994, **215**, 131; (*b*) A. L. Abuhijleh, C. Woods, E. Bogas and G. L. Guenniou, *Inorg. Chim. Acta*, 1992, **195**, 67; (*c*) M. R. Malachowski, M. G. Davidson and J. N. Hoffman, *Inorg. Chim. Acta*, 1989, **157**, 91; (*d*) M. R. Malachowski and M. G. Davidson, *Inorg. Chim. Acta*, 1989, **162**, 199; (*e*) R. Marion, N. M. Saleh, N. Le Poul, D. Floner, O. Lavastrec and F. Geneste, *New J. Chem.*, 2012, **36**, 1828.

14 E. Mijangos, J. Reedijk and L. Gasque, *Dalton Trans.*, 2008, 1857.

15 A. W. Smith, A. Camara-Artigas, M. Wang, J. P. Allen and W. A. Francisco, *Biochemistry*, 2006, **45**, 4378.

16 (*a*) A. Panja, M. Shyamal, A. Saha and T. K. Mandal, *Dalton Trans.*, 2014, **43**, 5443; (*b*) A. Panja, *Dalton Trans.*, 2014, **43**, 7760; (*c*) C. Mukherjee, T. Weyhermüller, E. Bothe and P. Chaudhuri, *C. R. Chim.*, 2007, **10**, 313; (*d*) C. Mukherjee, T. Weyhermüller, E. Bothe, E. Rentschler and P. Chaudhuri, *Inorg. Chem.*, 2007, **46**, 9895.

17 E. Gungor, H. Kara, E. Colacio and A. J. Mota, *Eur. J. Inorg. Chem.*, 2014, 1552.

18 G. M. Sheldrick, *Acta Crystallogr., Sect. A: Found. Crystallogr.*, 2008, **64**, 112.

19 O. V. Dolomanov, L. J. Bourhis, R. J. Gildea, J. A. K. Howard and H. Puschmann, *J. Appl. Crystallogr.*, 2009, **42**, 339.

20 L. J. Farrugia, *ORTEP-32 for Windows*, University of Glasgow, Scotland, 1998.

21 (*a*) L. Salmon, P. Thuéry, E. Rivière, J.-P. Costes, A. J. Mota and M. Ephritikhine, *New J. Chem.*, 2014, **38**, 1306; (*b*) B. K. Babu, A. R. Biju, S. Sunkari, M. V. Rajasekharan and J.-P. Tuchagues, *Eur. J. Inorg. Chem.*, 2013, 1444; (*c*) R. Papadakis, E. Rivière, M. Giorgi, H. Jamet, P. Rousselot-Pailley, M. Réglier, A. J. Simaan and T. Tron, *Inorg. Chem.*, 2013, **52**, 5824; (*d*) S. Mukherjee and P. S. Mukherjee, *Dalton Trans.*, 2013, **42**, 4019; (*e*) M. Sutradhar, M. V. Kirillova, M. F. C. G. da Silva, C.-M. Liu and A. J. L. Pombeiro, *Dalton Trans.*, 2013, **42**, 16578.

22 F. Zippel, F. Ahlers, R. Werner, W. Haase, H.-F. Nolting and B. Krebs, *Inorg. Chem.*, 1996, **35**, 3409.

23 S. Tsuruya, S.-I. Yanai and M. Masai, *Inorg. Chem.*, 1986, **25**, 141.

24 (*a*) A. I. Vogel, *Textbook of quantitative inorganic analysis*, Green and Co. Ltd., London, 1961, 3rd end, p. 366, Longmans; (*b*) A. Neves, L. M. Rossi, A. J. Bortoluzzi, B. Szpoganicz, C. Wiezbicki and E. Schwingel, *Inorg. Chem.*, 2002, **41**, 1788; (*c*) E. Monzani, L. Quinti, A. Perotti, L. Casella, M. Gullotti, L. Randaccio, S. Geremia, G. Nardin, P. Faleschini and G. Tabbi, *Inorg. Chem.*, 1998, **37**, 553.

